Nano Communication Networks 4 (2013) 53–64

Contents lists available at SciVerse ScienceDirect

Nano Communication Networks

journal homepage: www.elsevier.com/locate/nanocomnet

Characterization of molecular communications among implantable biomedical neuro-inspired nanodevices

Laura Galluccio [a,*], Sergio Palazzo [a], G. Enrico Santagati [b]

[a] Dipartimento di Ingegneria Elettrica, Elettronica ed Informatica, University of Catania, V.le A. Doria 6, 95125 Catania, Italy
[b] Department of Electrical Engineering, The State University of New York at Buffalo, NY, United States

ARTICLE INFO

Article history:
Received 12 January 2013
Accepted 7 March 2013
Available online 21 March 2013

Keywords:
Nanonetworks
Nanomachines
Neuronal communications
Neuronal noise
Channel capacity

ABSTRACT

In the next future nanodevices are expected to be implanted in the human body and communicate with each other as well as with biological entities, e.g. neuronal cells, thus opening new frontiers for disease treatment, especially in neurological therapy and for drug delivery. Moreover, considering that these nanoscale devices will be small in size, will have limitations in terms of energy consumption and processing and will be injected into a biological system, they will be not able to use traditional electromagnetic or acoustic communications paradigms: rather, they will employ communication schemes similar to those used by neuronal cells and based on molecule exchange. With respect to this, a theoretical work is required to identify the information bounds for nanoscale neuronal communications. In previous papers, achievable information rates of active and passive transport in molecular communication systems have been investigated in the hypothesis of considering two nanodevices which exchange information through molecules released by a transmitter and diffused according to a Brownian motion or using molecular motors. Stochasticity in the diffusion process of these molecules causes noise in the communication among these nanodevices. In this paper we address the derivation of information bounds by introducing a realistic neuron-like communication model which takes into account interactions among nanodevices that can be implanted in the human body and, like neurons, can be simultaneously connected through thousands of synapses. In particular, an accurate characterization of the communication channel is derived and the estimation of the capacity bounds is achieved.

In the next decade, treatment of neurological diseases (e.g. depression, Alzheimer's, epilepsy) and, in general, biomedical applications, are expected to rely on innovative nanomachine-to-neuron and nanomachine-to-nanomachine communication paradigms [1,31,32].

These paradigms will be concerned with interactions among both biological and non-biological entities. This implies that nanodevices have to exhibit the same communication behavior of biological entities, which otherwise would not be able to understand and correctly interpret the stimuli issued by nanodevices in their surrounding.

In this perspective, it is of paramount importance to characterize neuronal communication channels.

In a previous work [16] we have modeled the neuronal functioning with the aim of emulating the biological neurons' operation. In particular, we provided a block model of the subsystems composing a single neuron and described their functioning in terms of transfer functions, i.e. gain and phase. Then, by considering the cascade of the different blocks mimicking the global neuronal behavior, we observed that the overall neuron system can be modeled as a low pass filter with a cut off frequency around 3–4 kHz.

* Corresponding author. Tel.: +39 095 738 2384; fax: +39 095 738 2397.
E-mail address: laura.galluccio@dieei.unict.it (L. Galluccio).

1878-7789/$ – see front matter © 2013 Elsevier Ltd. All rights reserved.
http://dx.doi.org/10.1016/j.nancom.2013.03.001

This result has soundly confirmed recurrent evidences experienced in medical tests, which show that neurons typically filter neuronal stimuli in the range [0, 3] kHz [22].

In spite of this, the results in [16] still represent an intermediate step towards a comprehensive characterization of the communication channel among neurons and neuron-inspired nanomachines.

Specifically, when considering nanomachine-to-neuron communications one major aspect which should be investigated in the aim of estimating and maximizing the communication throughput is the *channel capacity*, and the associated information theoretical bounds have to be properly identified.

With respect to this, observe that the molecules' release involved in the nanomachine-to-neuron communication is subject to a high degree of stochasticity which has been proven to cause noise. However, it was shown that this stochastic behavior cannot be modeled by means of an additive Gaussian noise as traditionally assumed in the Shannon communication theory [25]. Therefore, an accurate study for the characterization of the molecular communications among biomedical neuro-inspired nanodevices should necessarily consider the distinctive peculiarities of the dynamics occurring in this specific context.

Previous literature in the field [2,3,23] has addressed the estimation of the achievable capacity in molecular systems which are typically assumed to employ calcium ions, liposomes or molecular motors to transport molecules carrying information. Specifically, in [2] the problem of defining a nanoscale information theory is raised. In [3] a molecular model is proposed to characterize transmitter–receiver communication and put it into relationship with environmental variables affecting the diffusion process, such as temperature, concentration of the emitted molecules and/or distance among the nanomachines. In [23] a mathematical expression for the molecular communication capacity when assuming that information relies on free diffusion of molecules is investigated. In this case also a parallelism between the thermodynamic entropy and the information entropy is presented and is used to identify the relationship with the system bandwidth and the transmitted power. In [11–14] some relevant studies on the achievable information rates of active and passive transport in molecular communication systems are presented. Specifically, a scenario where the information exchange between two nanodevices is achieved through molecules (i.e. vesicles) traveling from a sender to a receiver is considered. These molecules can passively diffuse according to a Brownian motion or can be actively transported using molecular motors. Stochasticity in the diffusion/transport process is considered as a cause of noise in nanodevices communication and, accordingly, achievable information rates are estimated. A simulative study is also presented to compare Brownian motion and molecular motors performance. Finally, in [20], a simulative investigation on the achievable information rate by modeling noise effects in molecular communications is discussed. In this case, noise is identified with information molecules persisting in the environment where they diffuse for a time longer than an assumed interval.

As compared to the work mentioned above, in this paper we focus on the specific context of nanodevices' interactions inspired by neuronal communication. In this case, we consider noise effects related to both the stochasticity of the ion channels as well as the excitatory and inhibitory signals due to thousands of synapses strictly interacting which have been experimentally observed to be the major sources of fluctuations and spontaneous firing (i.e. excitation) in neurons.

When assuming that a nanomachine stimulates a neuron, one is interested in estimating the maximum of the mutual information which can be exchanged among the two nodes. This consideration applies even more in case of nanomachines communicating with each other. In fact these devices, once injected into the human body, could either communicate with biological entities (e.g. neurons) or not (i.e. with other nanomachines), but are anyhow immersed in an environment full of molecules (e.g. neurotransmitters) which effects their behavior.

The communication capacity can be estimated by modeling the probability density function (pdf) of the signal received at a neuron/nanomachine, given the one that was transmitted by the sender. In order to estimate this capacity, in this paper we will first recall some basics on the neuron structure and introduce a noise characterization at the neuronal synapses. Then we will use this noise model to calculate also the bit error rate. Finally, the ratio between the mutual information and the average transmission time Ψ and the bits-per-joule performance Γ are estimated.

The rest of this paper is organized as follows. In Section 1 we briefly describe the physiological basics of the neuron structure. In Section 2 we illustrate the neuronal model which has to be properly considered when the neuron is not simplistically described as a single entity with a concentrated parameter model, but is assumed to consist of a chain of N compartments along which the signals propagate. Then, in Section 3 we discuss the mathematical model of the neuronal noise. In Section 4 we estimate the channel capacity, the bit error rate and the bits-per-joule. In Section 5, we present the results of the numerical evaluation. Finally, in Section 6, some conclusions are drawn.

1. The neuron structure in a nutshell

A neuron is a complex cell. Its structure is illustrated in Fig. 1(a). It consists of a cell body implementing the system logic, called *soma*, a cell extension used as the output interface, named *axon*, and a set of thin structures arising from the cell body which can be identified as the input interfaces, called *dendrites*. A cellular membrane separates the internal cytoplasm from the extracellular medium. Across the cellular membrane there exists an ion gradient which causes a diffusion process fundamental for cell activity. As an example, there is typically an excess of sodium and chlorine ions Na^+ and Cl^- outside, and potassium ions K^+ inside. This difference in ion concentrations induces a voltage difference denoted as *resting potential* E_r. The ion gradient is maintained through an active transport system which continuously contrasts passive diffusion due to chemical

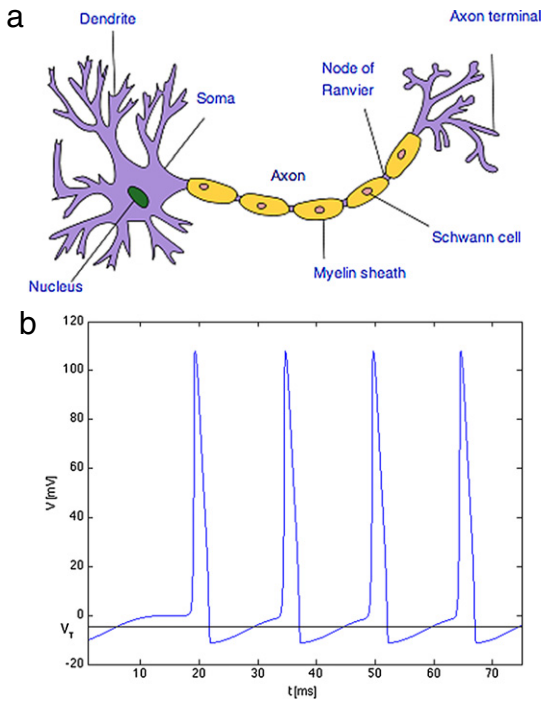

Fig. 1. (a) Neuron structure and (b) membrane potential variation in case of iterated action potential occurrence.

equilibrium. Existence of a stable ion gradient between the internal and external parts of a cell leads to a variation in the membrane potential. It is possible to efficiently modulate the membrane potential amplitude simply varying the membrane permeability to specific ions.

The cellular membrane consists of a phospholipid bilayer with embedded proteins able to perform basic functionalities for cell activity. The main membrane proteins can be classified as *membrane receptors* and *ion channels*.

Membrane receptors can bind only to certain molecules, called *ligands*, thus causing the activation of a specific biological or chemical effect. *Ion channels* form aqueous pores in the phospholipid bilayer that allow ion exchange through the membrane. Obviously the voltage difference at the cellular membrane can be modulated by varying the number of open ion channels after the binding between the membrane receptors and the ligands.

When specific cells, such as neurons, are stimulated by external inputs (e.g. during neuronal excitation), basically two types of responses take place: passive and active. Experimental tests show that, if electrical current flows through the cell membrane, this reacts passively like an *RC* parallel circuit where R is the resistive component of ion transportation through ion channels at the membrane, and C represents the membrane capacitive component associated to the dielectric properties of the phospholipid bilayer.

In addition to a passive response, an excitable cell, such as a neuron, also exhibits an active response, called *action potential* or *spike*. If the external stimulus is strong enough to make the membrane potential rise up to a threshold value V_T, a depolarization occurs, and the response activates an *all-or-none* event in which the electrical membrane potential of the cell rapidly raises and then falls. The reason for this behavior is that when the sodium channels are open, they allow an incoming flow of sodium ions, which changes the electrochemical gradient; this in turn leads to a depolarization in the membrane potential which causes more sodium channels to open, producing a greater electric current. The process goes on until all the available sodium channels are open, causing a rise in the membrane potential. Due to the incoming flux of sodium ions, the membrane reverses its polarity and the sodium channels then rapidly inactivate. When the sodium channels close, ions can no longer enter the neuron and are left out of the membrane. Potassium channels are then activated making the electrochemical gradient return to the initial resting state. The time needed to allow this transition back to the resting state is called the *refractory period* and represents the delay that should elapse before a new depolarization of the membrane potential can take place. An example of membrane potential variation is shown in Fig. 1(b) in case of iterated action potential occurrence.

2. Compartmental model of the neuron

In order to model the neuron-like behavior of a nanodevice, let us consider the equivalent *compartmental membrane model* of a neuron as presented in [24]. A compartment is a portion of the dendritic tree. The latter is divided into small cylindric sections with an approximatively uniform membrane potential. Each compartment is characterized by its capacity and transversal conductivity. The compartmental model allows to describe in much detail the spatio-temporal pattern of inputs applied to multiple regions of a neuron. More specifically, the model in [24] accounts for the effects of signal propagation through dendritic trees when assuming that both excitatory and inhibitory signals are applied at various locations of the dendritic tree, either simultaneously or not, as an effect of the external inputs. The branched dendritic tree is modeled as an equivalent cable of passive uniform membrane. The distribution of the membrane potential along the length of this branch follows the cable equation [28] and the description is accurate in the hypothesis that the branch diameters satisfy the specific relationship that the sum of the power 3/2 of the children branches' diameters is equal to the power 3/2 of the parent branch diameter. If this relationship is satisfied, it has been demonstrated that the use of a finite length cable is a good model to represent ideal dendritic trees.

The reference compartmental model is depicted in Fig. 2. More specifically, in Fig. 2(a) we show an example of dendritic tree; in Fig. 2(b) we represent the membrane equivalent circuit for each compartment.

According to the compartmental model [24], the membrane potential at the i-th compartment can be described through a system of ordinary linear first-order differential

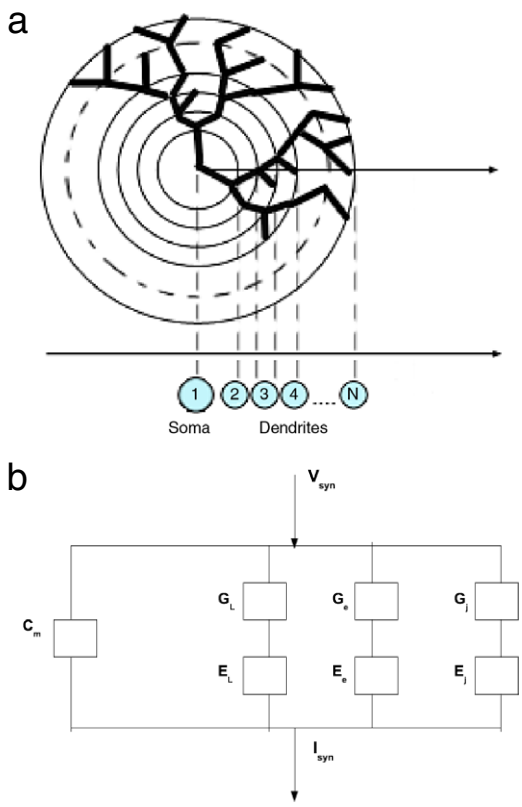

Fig. 2. Compartmental model.

equations in the form:

$$\begin{cases} \dfrac{dV_{\text{syn},i}}{dt} = \displaystyle\sum_{h=1}^{N} \mu_{i,h} V_{\text{syn},h} + f_i \\ f_i = \dfrac{(\varepsilon_i + \beta_i \gamma_i + \chi_i)}{\tau_i} \\ \mu_{h,j} = -\dfrac{\varepsilon_h + \gamma_h + \chi_h}{\tau_h} - \displaystyle\sum_{j \neq h} \mu_{h,j} \quad h = j \\ \mu_{h,j} = \dfrac{1}{\tau_h \Delta z^2} \quad h = j+1,\ j-1 \\ \mu_{h,j} = 0 \quad \text{otherwise.} \end{cases} \tag{1}$$

Observe that in the above equations, in case of a straight chain of compartments modeled as a cylinder, Δ_z is the equivalent increment of each compartment.

In the above set of equations, for the i-th compartment, the relevant parameters are defined as follows:

- $\varepsilon_i = [G_e/G_L]_i$
- $\beta_i = [E_j]_i$
- $\gamma_i = [G_j/G_L]_i$
- $\chi_i = 1$
- $\tau_i = [C_m/G_L]_i$

where G_e is the equivalent conductance associated to the application of an external excitatory signal of electromotive force E_e at a specific compartment i; G_L is the equivalent leakage conductance accounting for resistive effects of the neuron membrane; G_j is the equivalent conductance associated to the application of an external inhibitory signal of electromotive force E_j at a specific compartment i; C_m is the equivalent capacitor modeling the capacitive effects of the membrane; E_L is the leakage electromotive force which considers the potential at which the leakage current due to chloride ions goes to zero.

Observe that in the above system all values of the potentials are estimated as the difference with respect to the resting potential E_r and normalized with respect to the difference $E_e - E_r$.

The synaptic membrane potential at the first compartment (i.e. the soma), $V_{\text{Syn},1}$, identifies the value of the synaptic voltage at the backward end of the dendritic tree. This is the voltage which propagates through the axon and causes neurotransmitter emission at the synapses.

3. Noise in neuronal communications

Neuronal activity is subject to stochasticity due to the ion channel functioning. This can be properly accounted in terms of noise sources [19,27] added to the equivalent circuit. In the literature there has been a great effort to understand and classify neuronal noise and derive some conclusions on how the dynamics of the action potential at neurons are influenced by noise. The main types of neuronal noise can be summarized as follows.

- *Ion conductance noise*: The ion conductance noise is related to the thermal fluctuations incurred by the ion channels. Each channel can be in one of two states: open or closed. In the open state, the ion channel is active and behaves like a pore allowing specific types of ions to migrate through the membrane, under the influence of an electrochemical gradient. However, it has been experimentally observed by Neher et al. [21] that each channel behaves independently from the others as a stochastic element due to the thermal fluctuations mentioned above. Accordingly, the simple deterministic membrane model proposed by Hodgkin and Huxley [18], the so called HH model, should be modified to take into account this stochasticity. This noise source will be considered in Section 3.1.
- *Synaptic bombardment noise*: Noise is related to the myriad of simultaneously active synapses that a neuron forms with other cells. Some models introduced in the past [4,5,9] stated that this background activity negatively acts on cellular responsiveness, thus reducing it. On the contrary, a more recent work [17] showed that the voltage fluctuations of background activity also have an impact on cellular responsiveness. In fact, in the presence of background activity with voltage fluctuations, responses to inputs that would be subthreshold in quiescent conditions can be produced. This challenges the traditional idea that neurons with low input resistance are characterized by low responsiveness. This noise source will be considered in Section 3.2.
- *Shot noise*: During ion channel opening, ions migrate in a stochastic way. Accordingly, this introduces fluctuations which can be identified with channel shot noise. Usually the effect of this noise is considered marginal as compared to other noise sources [7].

- *Ion pumps noise*: The presence of ion pumps which employ energy for active ions' transport across a membrane electrochemical gradient implies a fluctuation in the membrane voltage. However, the effect of this noise is usually disregarded in comparison with other noise sources [7].

In the following we will focus our attention on modeling the major noise sources on signal propagation in a neuron. In particular, we will illustrate how considering the effects of the ion conductance noise and the synaptic bombardment noise affects the parameters of the membrane equivalent circuit.

3.1. Ion conductance noise modeling

Traditionally, the membrane voltage variation in a neuron is described using the deterministic HH model as described in Eq. (1). Together with this, we propose to combine a neuron compartmental model in such a way as to assume that the membrane voltage variation at each of the considered compartments can be expressed similarly to an *RC* circuit. When specifically considering the sodium and potassium leakage conductances associated to the ion channels, G_{Na} and G_K, respectively, the system in Eq. (1) can be rewritten as

$$\begin{cases} \dfrac{dV_{syn,i}}{dt} = \displaystyle\sum_{h=1}^{N} \mu_{i,h} V_{syn,h} + l_i \\ l_i = \dfrac{(\varepsilon_i + \beta_i\gamma_i + \chi_i + \delta_i\phi_i + \lambda_i\xi_i)}{\tau_i} \\ \mu_{h,j} = -\dfrac{\varepsilon_h + \gamma_h + \chi_h + \delta_h + \lambda_h}{\tau_h} \\ \qquad - \displaystyle\sum_{j\neq h} \mu_{h,j} \quad h = j \\ \mu_{h,j} = \dfrac{g_{h,j}}{c_h} = \dfrac{g_{j,h}}{c_i} \quad h = j+1,\ j-1 \\ \mu_{h,j} = 0 \quad \text{otherwise.} \end{cases} \tag{2}$$

In the above set of equations, for the i-th compartment, the additional relevant parameters not already discussed for Eq. (1) are:

- $\delta_i = [G_{Na}/G_L]_i$;
- $\phi_i = [E_{Na}]_i$;
- $\lambda_i = [G_K/G_L]_i$;
- $\xi_i = [E_K]_i$;

where E_{Na} and E_K are the sodium and potassium leakage reversal voltages, respectively. Observe that each of the conductances G_{Na} and G_K depends on three main factors: the number of ion channels for sodium and potassium per membrane surface unit, N_{Na} and N_K, the number of these channels that are open at time t, and the individual channel conductances Γ_{Na} and Γ_K. Accordingly, the higher the percentage of active channels and/or the number of channels, the higher the conductances. For sodium and potassium, the number of open channels at time t is traditionally denoted in the literature as m^3h and n^4, respectively, and depends on the membrane voltage itself. Moreover, m, n and h have to satisfy the following set of equations:

$$\begin{cases} \dfrac{dm}{dt} = \alpha_m(1-m) - \beta_m m \\ \dfrac{dn}{dt} = \alpha_n(1-n) - \beta_n n \\ \dfrac{dh}{dt} = \alpha_h(1-h) - \beta_h h. \end{cases} \tag{3}$$

In [8] an evolution of the HH model is also introduced. This enhanced model assumes stochastic states for the potassium and sodium channels. In particular, for the potassium channels, $4 \cdot N_K$ two-states elements – specifically proteins – are considered, where each element can be either open or close. Elements are grouped in sets of four, thus yielding to N_K single channels. If all four elements of any single channel are open at time t, the corresponding channel is assumed to be open and has a conductance Γ_K; alternatively, the channel is regarded as non conducting. The total conductance at time t is given by the sum of the conductances of all conducting channels [15]. For the sodium channels, similar considerations apply with each channel composed of four elements out of which three are m elements and one is an h element. Also the probabilities that a sodium channel remains open or closed can be similarly computed, by using parameters α_m, α_h, β_m and β_h.

Actually, in real biological systems both the original and enhanced HH models showed to be not suitable to take into account the stochastic channel behavior and, therefore, a stochastic variant of the HH model has to be considered [15]. More specifically, a set of first-order differential equations which describe the time evolution of the probability of the system to occupy each of a discrete set of states is needed. This is the – so called – master equation [30] for potassium and sodium channels which considers the possibility to have a limited number of channels N_K and N_{Na}. The derivation of the master equation which gives the transition probabilities and the probability distribution function is complex but can be simplified into the Fokker–Planck equations [30] in the hypothesis that the number of sodium and potassium channels, N_{Na} and N_K, is very high.

Nevertheless, solving the Fokker–Planck equations can be still very complex. So, a further simplified Langevin description [30] can be associated to the Fokker–Planck equations. The Langevin description uses stochastic ordinary differential equations (and not partial, like those in the Fokker–Planck model). The equivalent Langevin model accordingly becomes

$$\begin{cases} \dfrac{d}{dt}m = \alpha_m(1-m) - \beta_m m + g_m(t) \\ \dfrac{d}{dt}n = \alpha_n(1-n) - \beta_n n + g_n(t) \\ \dfrac{d}{dt}h = \alpha_h(1-h) - \beta_h h + g_h(t) \end{cases} \tag{4}$$

where $g_n(t)$, $g_m(t)$ and $g_h(t)$ are statistically independent white Gaussian noises with zero mean and autocorrelation

given as follows:

$$\begin{cases} \langle g_n(t)g_n(t')\rangle = 2\dfrac{\alpha_n\beta_n}{N_{\mathrm{K}}(\alpha_n+\beta_n)}\delta(t-t') \\ \langle g_m(t)g_m(t')\rangle = 2\dfrac{\alpha_m\beta_m}{N_{\mathrm{Na}}(\alpha_m+\beta_m)}\delta(t-t') \\ \langle g_h(t)g_h(t')\rangle = 2\dfrac{\alpha_h\beta_h}{N_{\mathrm{Na}}(\alpha_h+\beta_h)}\delta(t-t'). \end{cases} \quad (5)$$

Eqs. (4) and (5), when substituted in (2), provide the stochastic version of the HH model with $G_{\mathrm{K}} = \Gamma_{\mathrm{K}}N_{\mathrm{K}}x'$ and $G_{\mathrm{Na}} = \Gamma_{\mathrm{Na}}N_{\mathrm{Na}}y'$, where x' and y' are the quantities n^4 and m^3h discussed above.

3.2. Synaptic bombardment noise modeling

In real biological systems, where each neuron has thousands of synapses simultaneously active with a multitude of neurons in its proximity, nanodevices mimicking neuronal behavior should be modeled so as to account for these interactions.

Accordingly, in [10] a conductance model has been assumed to approximate the synaptic background activity at any single compartment. More specifically, the synaptic current at the i-th compartment is represented as consisting of two terms: the one accounting for the excitatory signal, and the other for the inhibitory signal. Specifically,

$$I_{\mathrm{syn},i} = g_e(t)(V-E_e) + g_j(t)(V-E_j) \quad (6)$$

where E_e and E_j (mV) are the excitatory and inhibitory reversal potentials, respectively, and $g_e(t)$ and $g_i(t)$ are time-dependent excitatory and inhibitory conductances which are approximated as a one-variable stochastic process similar to the Ornstein–Uhlenbeck process [29] and thus satisfy the following system

$$\begin{cases} \dfrac{dg_e(t)}{dt} = -\dfrac{1}{\tau_e}[g_e(t)-g_{e0}] + D_e^{1/2}\chi_1(t) \\ \dfrac{dg_j(t)}{dt} = -\dfrac{1}{\tau_j}[g_j(t)-g_{j0}] + D_j^{1/2}\chi_1(t). \end{cases} \quad (7)$$

In Eq. (7) g_{e0} and g_{j0} are the average conductances, τ_e and τ_j are appropriate time constants as assumed in [10], D_e and D_j are the noise diffusion coefficients in the case of excitatory and inhibitory signals, respectively, and χ_1 and χ_2 are normalized standard white Gaussian noises used to model the stochasticity of the synaptic bombardment noise.

Accordingly, the membrane potential equation at each compartment, when accounting for both the ion conductance and the synaptic bombardment noises, will be in the form

$$\frac{dV_{\mathrm{syn},i}}{dt} = \frac{1}{C_m}\cdot[-I_{\mathrm{Na}} - I_{\mathrm{K}} - I_{\mathrm{syn},i} - G_L(V-E_L)] \quad (8)$$

where $I_{\mathrm{Na}} = G_{\mathrm{Na}}(V-E_{\mathrm{Na}})$ and $I_{\mathrm{K}} = G_{\mathrm{K}}(V-E_{\mathrm{K}})$.

4. Information bounds

In this section we will estimate the information bounds of the noisy communication channel among nanodevices or nanodevices and neurons according to the model illustrated in the previous sections. Specifically, in Section 4.1 we will calculate the capacity and the bit error rate and in Section 4.2 we will evaluate the bits-per-joule performance.

4.1. Channel capacity and bit error rate

Let us consider a nanodevice interacting with another nanodevice using a molecular communication mechanism. We assume they are connected through an ideal discrete memoryless channel. Specifically, a source (i.e. the transmitter) has a set of possible transmission symbols $\mathbf{X}$ and transmits a symbol $X \in \mathbf{X}$ per channel use. Due to the noise introduced by the channel, the receiver might not receive the symbol X correctly. Let us denote as $\mathbf{Y}$ the set of possible symbols that the destination can receive and Y the symbol in $\mathbf{Y}$ that the destination receives per each channel use.

We assume that a binary communication occurs[1] and only two symbols can be transmitted, that is, $\mathbf{X} = 0, 1$. According to the way information is propagated throughout a neuron, we also assume that symbols are coded into an action potential emission in case of a bit 1, and no action potential emission in case of a bit 0. In the following we calculate the ideal capacity of the communication channel, that is, the maximum rate at which any system can reliably transmit information over this noisy channel.

According to the Shannon theory [26], the channel capacity is defined as:

$$C = \max_{p(x)} I(X;Y) = \max_{p(x)} \sum_{k=0}^{1}\sum_{j=0}^{1} p(x_j,y_k)\log_2\frac{p(y_k|x_j)}{p(y_k)} \quad (9)$$

where $I(X;Y)$ is the mutual information, and the two possible transmitted and received symbols are $\{x_0 = 0, x_1 = 1\}$ and $\{y_0 = 0, y_1 = 1\}$, respectively.

In Eq. (9) the probabilities $p(y_k|x_j)$, $p(x_j,y_k)$ and $p(y_k)$ have to be calculated.

To this purpose, let us consider the stochastic process $V_{RX}(t)$, representing the membrane potential value at the receiver. In case of a transmitted bit 0 or 1, it is expected that $V_{RX}(t) < V_T$ or $V_{RX}(t) \geq V_T$, respectively, where V_T is the threshold value introduced in Section 1.

However, due to the noise effect, the V_{RX} can have fluctuations and, thus, given that a symbol 0 or 1 is transmitted, the conditioned pdf on Y has to be calculated. The calculation of the probabilities $p(y_k|x_j)$, $p(x_j,y_k)$ and $p(y_k)$ then can be done numerically in a rather straightforward way.

Then, the channel capacity can be obtained by calculating the partial derivatives of the mutual information with respect to $p(x_0)$ and $p(x_1)$, where $p(x_0)$ is the probability that the source emits a symbol 0 and $p(x_1)$ is the probability that the source emits a symbol 1.

Finally, observe that the bit error rate (BER), that is, the probability that the binary signal is corrupted by errors due

[1] In principle, also multiple level coding could be taken into account. However, due to the nature of the elementary entities involved, considering they use a simple binary encoding looks a reasonable assumption for this channel capacity analysis.

to the noise, can be calculated as:

$$\mathrm{BER} = p(y_1|x_0)p(x_0) + p(y_0|x_1)p(x_1) = p(x_0) \times [p(y_1|x_0) - p(y_0|x_1)] + p(y_0|x_1). \quad (10)$$

We will see in Section 5 that the values of $p(y_j|x_k)$ needed for the estimation of the BER can be obtained by performing a curve fitting of the pdf of Y given X.

4.2. Bits-per-joule performance

When a bit 1 is issued, considering that this is associated to an action potential generation, the presence of excitatory and inhibitory signals has no significant impact on the neuronal firing, and thus, the bit error probability is expected to be negligible. When a bit 0 is issued, on the contrary, the presence of excitatory and inhibitory signals can lead to an increase in the firing and, thus, results in a higher error rate. Therefore, the communication channel between the two nanomachines is basically a binary asymmetric channel. In this channel, upon increasing the probability to issue a bit 0, the BER increases. So the transmission of a bit 0 can be somehow regarded as detrimental to the system communication reliability. On the other hand, however, in spite of the increase in the bit error rate associated to the emission of a bit 0, a decrease in the transmission power is achieved.

Also, an interesting feature associated to the emission of bit 0 is the possibility of increasing the transmission rate. In fact, the transmission of a bit 1 implies propagation of the action potential, and the action potential cannot be issued at any rate since a refractory period is met, as discussed in Section 1. When assuming that nanomachines communicate exploiting a neuronal communication paradigm, it is evident that the refractory period should be accounted as a limiting factor in the capacity of the system. So, upon transmitting a bit 1 encoded into an action potential emission, no more than one bit every Δ_1 seconds can be issued. On the contrary, the transmission of a bit 0 can theoretically occur with an infinite rate, being not limited by any refractory period. In this case the only constraint is associated to the receiver detection time, denoted as Δ_0.

Actually, a tradeoff has to be identified between the need to increase the number of bits transmitted per each channel use and per each unit of energy. To this purpose, in this section we will consider the metric denoted as Ψ and defined as the ratio between the mutual information and the average bit transmission time. More specifically, Ψ is defined as

$$\Psi = \frac{I(X;Y)}{p(x_0)\cdot\Delta_0 + [1-p(x_0)]\cdot\Delta_1}. \quad (11)$$

The average energy consumption associated to the transmission of a symbol can be written as

$$\hat{\mathcal{E}} = [1-p(x_0)]\cdot\mathcal{E}_1 + p(x_0)\cdot\mathcal{E}_0 \quad (12)$$

where $\mathcal{E}_1$ and $\mathcal{E}_0$ are the energy consumptions associated to the transmission of bit 1 and bit 0, respectively.

Finally, the bits-per-joule performance Γ will be

$$\Gamma = \frac{\Psi}{\hat{\mathcal{E}}} = \frac{I(X;Y)}{p(x_0)\Delta_0 + (1-p(x_0)\Delta_1)} \times \frac{1}{[1-p(x_0)\mathcal{E}_1] + p(x_0)\mathcal{E}_0}. \quad (13)$$

The Γ metric estimates the amount of information which can be transferred while taking into consideration both the energy consumption and the achievable bit rates.

5. Numerical results

In this section we provide a numerical estimation of the metrics illustrated above, i.e. channel capacity, bit error rate, and bits-per-joule performance. The numerical results have been obtained using the Mathworks Matlab Simulink tool and developing a neuronal model implementing the theoretical framework discussed in the previous sections.

We have specifically implemented a multi-compartmental neuronal model with $N = 10$ compartments, in the aim of achieving a good tradeoff between need of fitting with realistic data and reduction in complexity. In fact, it was shown that considering $N = 10$ compartments modeling the cable between the soma, identified as the compartment 1, and each of the dendritic compartments enumerated from 2 to $N = 10$, provides a good approximation in case of very simple types of neurons, such as the pyramidal cells of the cerebral cortex[2] [6].

To illustrate the Simulink model, in Fig. 3, as an example, a snapshot of the compartment 1 (i.e. the soma) is shown. Other compartments are similarly modeled.

Both the ion conductance and the synaptic bombardment noise have been considered in the model. Specifically, ion conductance noise generators, I_{Na} and I_{K}, are accounted through blocks *Na Channel* and *K Channel*, respectively; synaptic bombardment noise generators, I_e and I_j, are accounted through blocks *Excitatory* and *Inhibitory*, respectively.

To investigate the effects of the noise on the neural communication, three different scenarios have been considered and compared. The first is an ideal scenario which refers to a neuron in isolation, and no noise generators. The second and third ones are more realistic scenarios where a neuron is interconnected to a dense neuronal network, and noise sources are accounted by considering the simultaneous presence of ion conductance noise and synaptic bombardment noise. The difference between the second and the third scenarios lies in the specific features of the neuronal pyramidal cells we have considered, which in the former belong to the Layer III, in the latter to the Layer VI [10].[3]

Moreover, as regards the synaptic bombardment noise, we have specifically considered three cases: (i) only excitatory signals are applied, (ii) only inhibitory signals are applied and (iii) both inhibitory and excitatory signals are applied together.

The ion conductance noise and the synaptic bombardment noise parameter values we have assumed in our simulations are reported in Tables 1 and 2, respectively.

[2] Pyramidal cells are a type of cortical neurons. About 3/4 of cortical cells are pyramidal. They are characterized by a triangular-shaped body, a variable length apical dendrite and other basal dendrites. The cerebral cortex consists of different layers of cells, typically denoted as ranging from Layer I to VI.

[3] This choice is motivated by the fact that the cells belonging to Layer III and VI exhibit parameter values, shown in Table 2, which typically are the minimum and maximum ones, respectively, as compared to those characterizing the other layers.

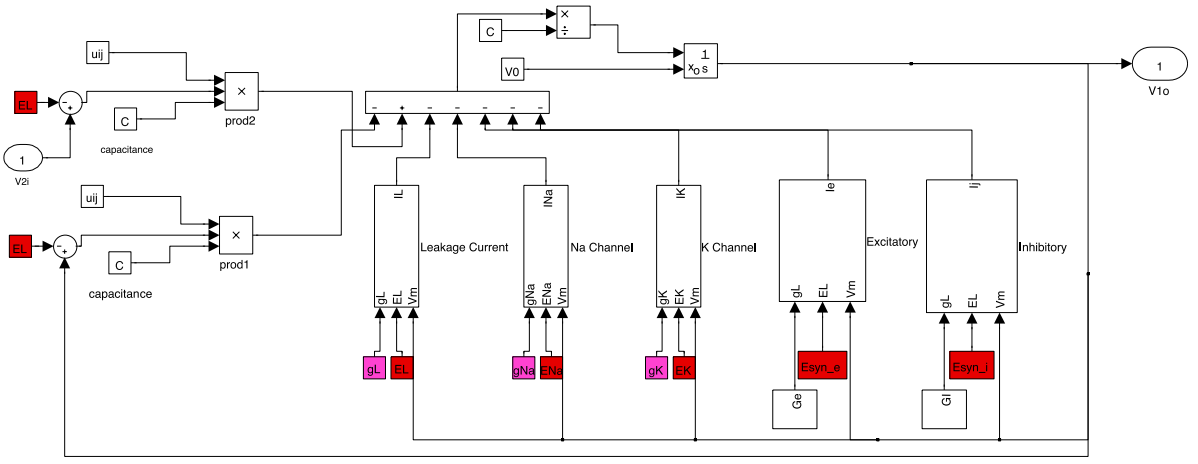

Fig. 3. Snapshot of the Simulink model for compartment 1.

Table 1
Ion conductance noise parameters for sodium and potassium channels.

α_m	$(25-V)/(10(\exp(25-V)-1))$
β_m	$4\exp(-V/18)$
α_h	$0.07\exp(-V/20)$
β_h	$1/(\exp(3-0.1V)+1)$
α_n	$(10-V)/(100(\exp(10-V)-1))$
β_n	$0.125\exp(-V/80)$

Table 2
Synaptic bombardment noise parameters for Layer III and Layer VI pyramidal cells.

Layer	III	VI
g_{e0} (μS)	0.006	0.012
σ_e (μS)	0.0019	0.003
τ_e (ms)	7.8	2.7
g_{j0} (μS)	0.044	0.057
σ_j (μS)	0.0069	0.0066
τ_j (ms)	8.8	10.5

In Fig. 4(a), (b) we show the mutual information and the bit error rate as a function of the probability to issue a symbol 0, $p(x_0)$, in the three scenarios illustrated above, and in the case that only excitatory signals are applied.

It is clearly evident that the impact of excitatory signals is not negligible. In particular, when they are applied the mutual information decreases as compared to the ideal case where the maximum is reached when the probability of issuing a symbol 0 is 0.5. This is because in the ideal case (i.e. when no noise is assumed) we have a binary symmetric communication channel where, as well known, the mutual information is maximized for $p(x_0) = 0.5$. On the contrary, incorporating the noise effects results in a binary asymmetric communication channel. This implies that the mutual information can be maximized for lower values of $p(x_0)$. Observe also that, as soon as we move from Layer III to Layer VI, the excitatory effects are almost doubled and consequently the mutual information decreases. Moreover, considering that the excitatory effect results in an increased probability to misinterpret the bit 0 as a bit 1 at the receiver, the mutual information can only be maximized by decreasing the probability to issue a bit 0, $p(x_0)$.

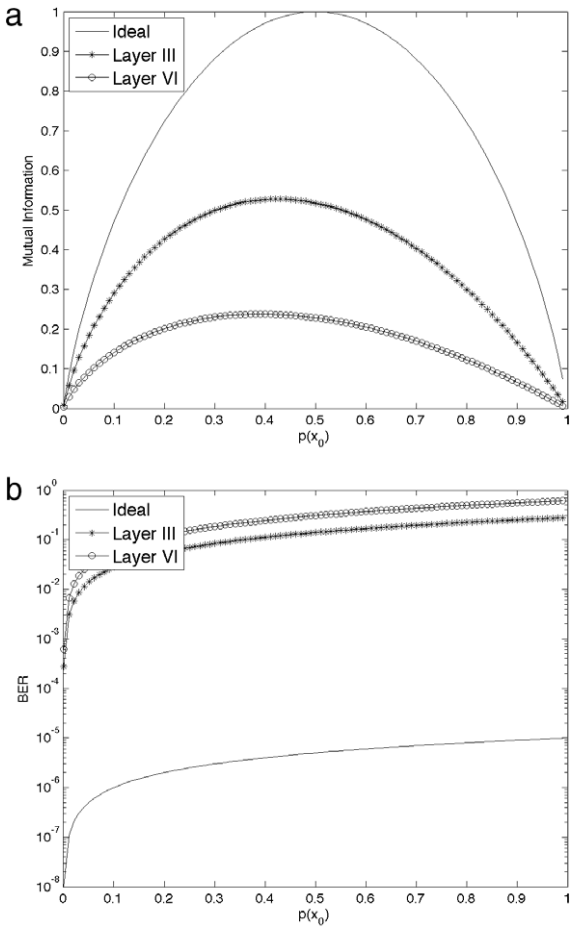

Fig. 4. Mutual information and bit error rate when only excitatory signals are applied.

As regards the BER, there is a remarkable difference in the performance of the Layer III and Layer VI cases, on one hand, and the ideal case on the other, although the trend of the three curves is similar. In Fig. 5(a) and (b) we show the mutual information and the bit error rate in the same

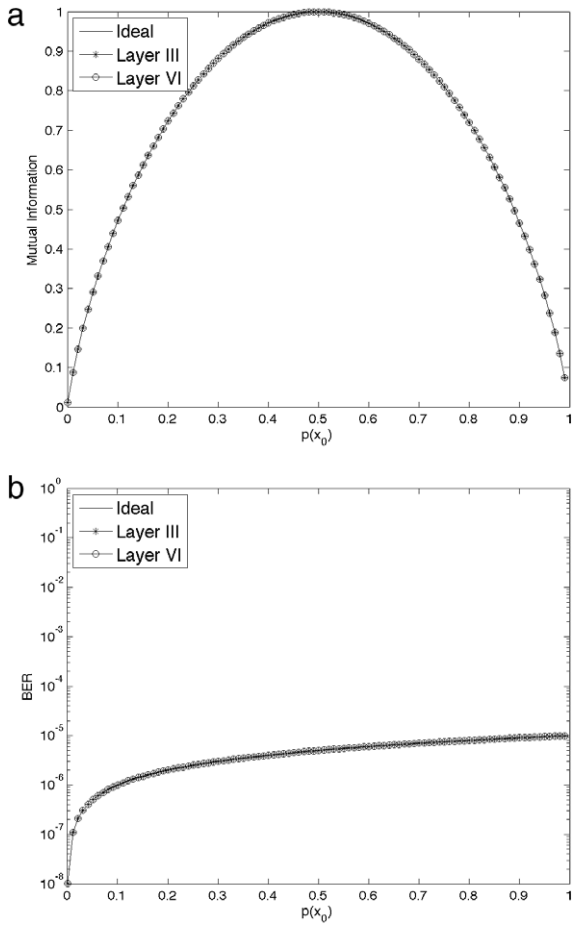

Fig. 5. Mutual information and bit error rate when only inhibitory signals are applied.

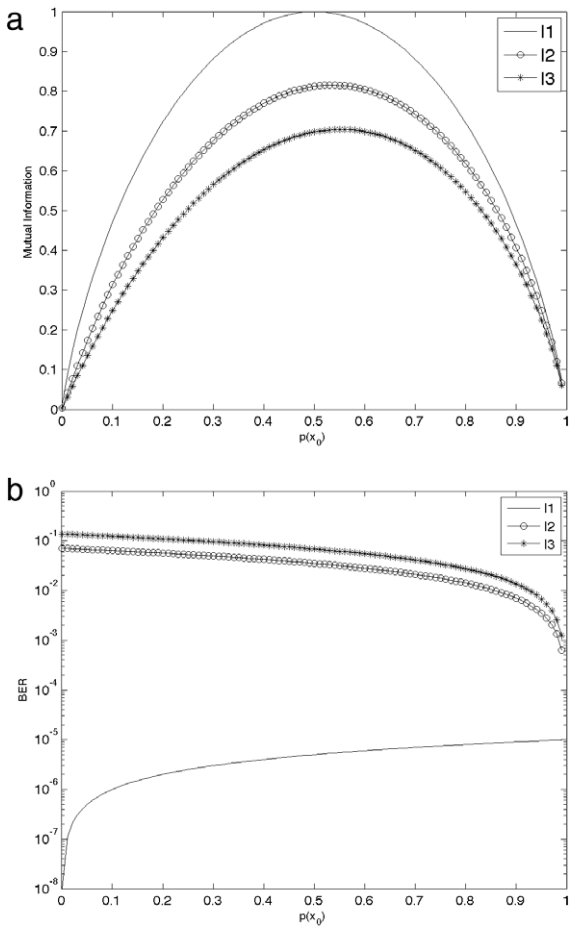

Fig. 6. Mutual information and bit error rate when only inhibitory signals are applied and when comparing different values of the inhibitory parameters.

conditions illustrated above but when only inhibitory signals are applied. The three curves for both the mutual information and the BER overlap: this is an evident clue that the impact of pure inhibitory signals is actually negligible. In fact, the expected effect would be to inhibit the action potential excitation. This effect is not observable when a bit 0 is issued since no action potential is emitted; on the other hand, in case of a bit 1 emission, this effect applies but does not play a significant role because the action potential firing is much more relevant. These considerations still apply even when moving from Layer III to Layer VI.

Also note that the BER is basically not impacted by a variation in the probability $p(x_0)$ at least for $p(x_0) > 0.2$.

In order to better investigate on the effects of inhibitory signals, in Fig. 6(a) and (b) we show the mutual information and the BER for cells of Layer VI, when assuming that only inhibitory signals are applied and changing the parameter values characterizing the synaptic bombardment noise. In particular, we compare the case $I1$, when the inhibitory parameters are those reported in Table 2, with the case $I2$ when g_{j0} and σ_j are doubled as compared to the values in Table 2, and the case $I3$ when g_{j0} and σ_j are increased five times as compared to the values in Table 2. We observe that an increase in the inhibitory effect causes a significant loss in terms of mutual information with a significant increase in the value $p(x_0)$ which maximizes it. This is due to the increase of the probability of misinterpreting the symbol 1. Similarly, an increase in the inhibitory effect leads to invert the trend in the BER which becomes decreasing, though taking higher values as compared to the case when the inhibitory effect is small.

In Fig. 7(a) and (b) we illustrate the case in which both excitatory and inhibitory signals are jointly considered. Applying the combination of these signals provides interesting and unexpected results due to the significant non linearities of the neuronal system. More in detail, we observe that, differently from the case of pure inhibitory signals, it is sufficient to consider a limited inhibitory contribution jointly acting with excitatory signals to have a dramatic increase in the mutual information. This applies to both the cases of Layer III and VI cells. Moreover, the joint effect is beneficial in the sense that the communication channel loses asymmetry. The BER is also positively impacted by this joint action since it decreases as compared to the case of pure excitatory signals.

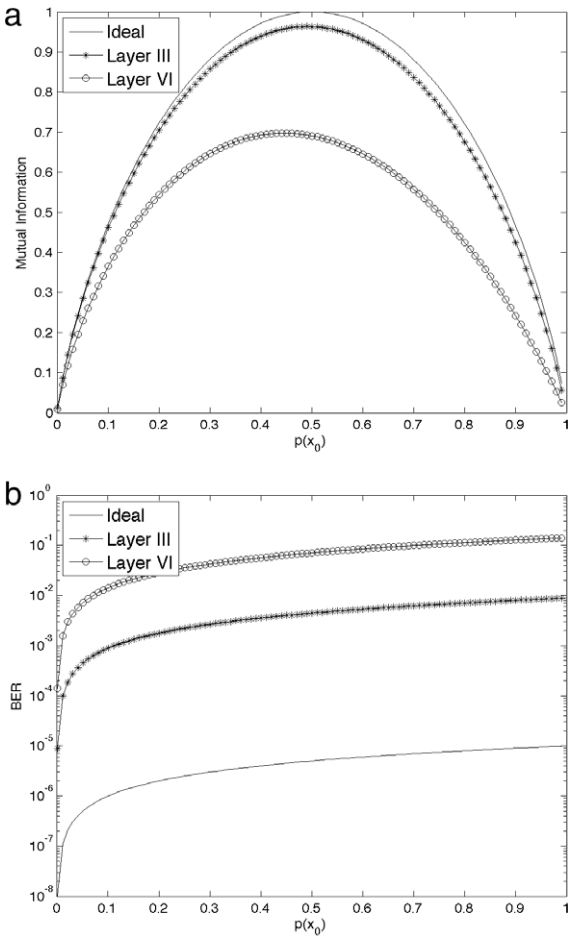

Fig. 7. Mutual information and bit error rate when both excitatory and inhibitory signals are applied.

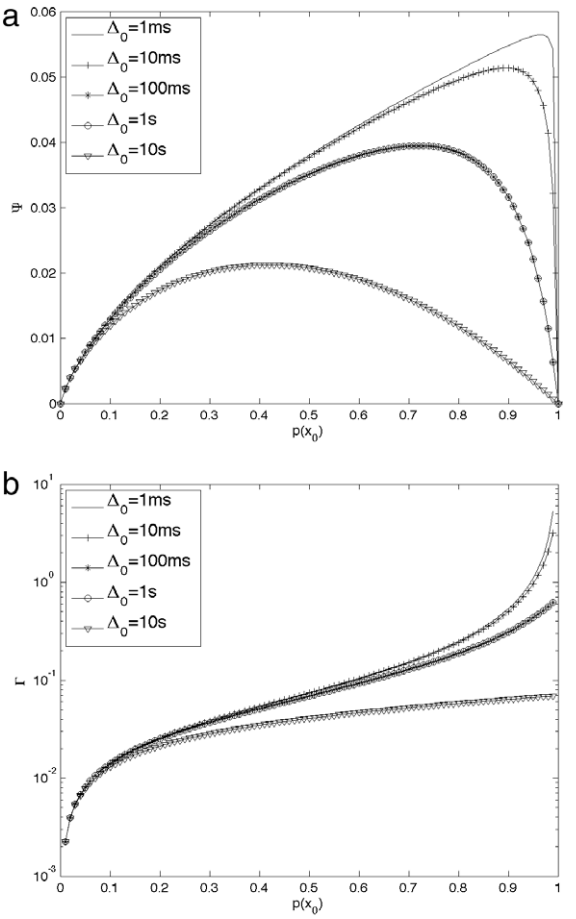

Fig. 8. Ψ function and Γ in a Layer VI cell with only excitatory signals applied for different values of Δ_0.

In Fig. 8(a) the ratio Ψ between the mutual information and the average bit transmission time is shown. In Fig. 8(b) the bits-per-joule performance, Γ, is plotted. Both Fig. 8(a) and (b) have been obtained when considering a Layer VI cell and investigating the conditions when only excitatory signals are applied. Different curves are shown as a function of the received detection time Δ_0. Note that, upon reducing Δ_0, the average bit transmission time decreases. However this effect becomes more relevant only for values of $p(x_0)$ higher than a certain threshold p_{Thr}, given that for $p(x_0) < p_{Thr}$ the curves are almost overlapped. This is because, when Δ_0 is fixed, for low values of $p(x_0)$ the denominator of Ψ in Eq. (11) is almost constant. Upon reaching the threshold, an additional increase in the probability $p(x_0)$ only results in a reduction in the mutual information as well as an increase in the dependence from the term $p(x_0)\Delta_0$ in the denominator of Ψ. As regards Γ, we observe that an increase in Δ_0 only causes a decrease in the amount of mutual information which can be encoded for a constrained energy. This is clearly a consequence of the fact that an increase in Δ_0 leads to a lower transmission rate.

When jointly considering the inhibitory and excitatory signals as shown in Fig. 9(a) and (b), significant increases in Ψ and Γ can be obtained, which are mainly related to the rise in the mutual information as discussed above.

Finally, in Fig. 10 we show the channel capacity as a function of both the probability p_{00} and p_{11} when simultaneously applying the inhibitory and excitatory signals. The plot confirms that the joint effect of applying inhibitory and excitatory signals mitigates the asymmetry in the communication channel.

6. Conclusions

In this paper we have addressed molecular communications in implantable biomedical neuro-inspired nanodevices. To this purpose we have modeled neuron communications and considered how they are impacted by noise. Also, we have identified the associated relevant information bounds for these nanoscale communication channels and observed that they are intrinsically asymmetric channels. These results open up new perspectives to study proper coding mechanisms for non-symmetric communication channels, and pave the way to the real application of unconventional neuro-inspired networking in the next future.

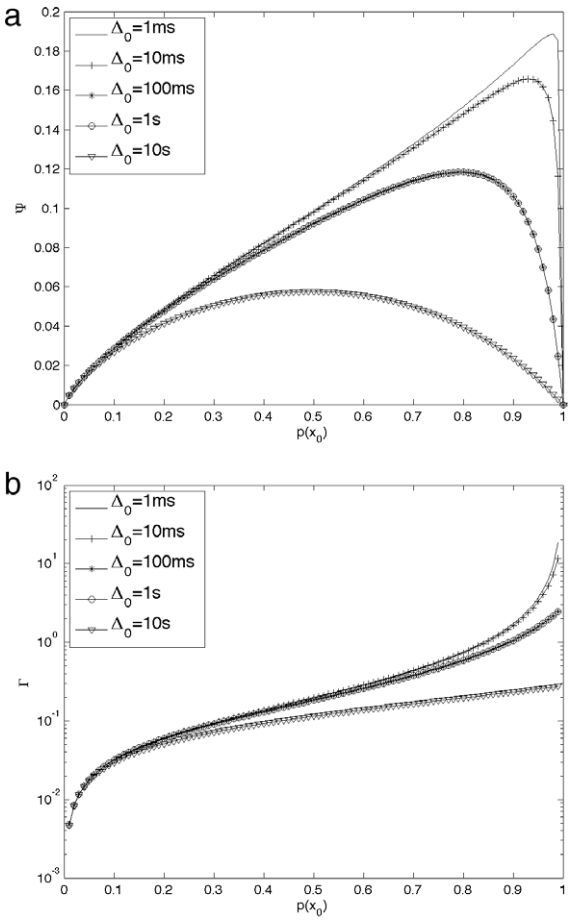

Fig. 9. Ψ function and Γ in a Layer VI cell with both excitatory and inhibitory signals applied for different values of Δ_0.

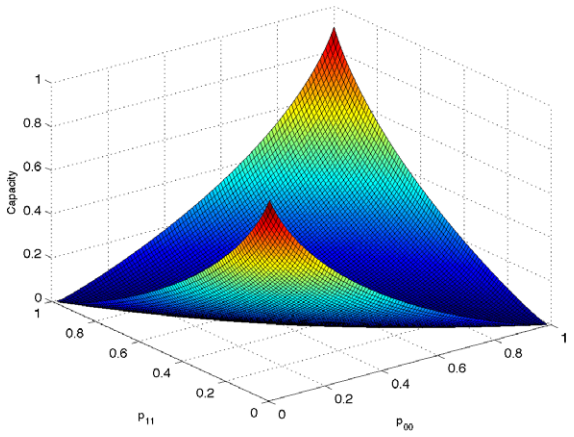

Fig. 10. Channel capacity as a function of both the probability p_{00} and p_{11} in a Layer VI cell with both excitatory and inhibitory signals applied.

References

[1] I.F. Akyildiz, F. Brunetti, C. Blazquez, Nanonetworks: a new communication paradigm, Elsevier Computer Networks 52 (12) (2008).

[2] G. Alfano, D. Miorandi, On information transmission among nanomachines, in: Proc. of 1st Int. Conference on Nanonetworks and Workshops, 2006. September.

[3] B. Atakan, O. Akan, An information theoretical approach for molecular communication, in: Proc. of 2nd Conf. on Bio-Inspired Models of Network, Information and Computing Systems, 2007. December.

[4] J.N. Barrett, Motoneuron dendrites: role in synaptic integration, Federation Proceedings 34 (5) (1975).

[5] O. Bernarder, R.J. Douglas, K.A. Martin, C. Koch, Synaptic background activity influences spatio-temporal integration in single pyramidal cells, National Academy of Sciences 88 (24) (1991).

[6] P.C. Bush, T.J. Sejnowski, Reduced compartmental models of neocortical pyramidal cells, Journal of Neuroscience Methods 46 (1993) 159–166.

[7] W.H. Calvin, C.F. Stevens, Synaptic noise and other sources of randomness in motoneuron interspike intervals, Journal of Neurophysiology 31 (4) (1988).

[8] L.J. DeFelice, A. Isaac, Chaotic states in a random world, Journal of Statistical Physics 70 (1) (1993).

[9] A. Destexhe, D. Paré, Impact of network activity on the integrative properties of neocortical pyramidal neurons in vivo, Journal of Neurophysiology 81 (1999).

[10] A. Destexhe, M. Rudolph, J.M. Fellous, T.J. Sejnowski, Fluctuating synaptic conductances recreate in-vivo-like activity in neocortical neurons, Neuroscience 107 (1) (2001).

[11] A.W. Eckford, Nanoscale communication with Brownian motion, in: Proc. of 41st Ann. Conf. Inform. Sci. Syst, 2007. March.

[12] A.W. Eckford, Achievable information rates for molecular communication with distinct molecules, in: Proc. of Bionetics, 2007. December.

[13] A.W. Eckford, N. Farsad, S. Hiyama, Y. Moritani, Microchannel molecular communication with nanoscale carriers: Brownian motion versus active transport, in: Proc. of IEEE International Conference on Nanotechnology, 2010.

[14] N. Farsad, A.W. Eckford, S. Hiyama, Y. Moritani, A simple mathematical model for information rate of active transport molecular communication, in: Proc. of IEEE MoNaCom, 2011. April.

[15] R.F. Fox, Y.-n Lu, Emergent collective behavior in large numbers of globally coupled independently stochastic ion channels, Physical Review 49 (4) (1994).

[16] L. Galluccio, S. Palazzo, G.E. Santagati, Characterization of signal propagation in neuronal systems for nanodevice-to-neurons communications, in: Proc. of IEEE MoNaCom, 2011. April.

[17] N. Ho, A. Destexhe, Synaptic background activity enhances the responsiveness of neocortical pyramidal neurons, The American Physiological Society Journal 84 (3) (2000).

[18] A.L. Hogkin, A.F. Huxley, A quantitative description of membrane current and its application to conduction and excitation in nerve, Journal of Physiology 177 (4) (1952).

[19] M.D. McDonnell, L.M. Ward, The benefits of noise in neural systems: bridging theory and experiment, Nature Reviews Neuroscience 12 (2011).

[20] M.J. Moore, T. Suda, K. Oiwa, Molecular communication: modeling noise effects on information rate, IEEE Transactions on Nanobioscience 8 (2) (2009).

[21] E. Neher, B. Sakmann, Single-channel currents recorded from membrane of denervated frog muscle fibres, Nature 260 (1976).

[22] A. Nunez, E. Carro, I. Torres-Aleman, Insulin-like growth factor *I* modifies electrophysiological properties of rat brain stem neurons, Journal of Neurophysiology 89 (6) (2003).

[23] M. Pierobon, I.F. Akyildiz, Information capacity of diffusion-based molecular communication in nanonetworks, in: Proc. of IEEE INFOCOM, Miniconference, Shanghai, China, 2011. April.

[24] W. Rall, Distinguishing theoretical synaptic potentials computed for different soma-dendritic distributions of synaptic input, Journal of Neurophysiology 30 (5) (1967).

[25] C.J. Rozell, D.H. Johnson, Examining methods for estimating mutual information in spiking neural systems, Neurocomputing 65 (2005).

[26] C.E. Shannon, Communication in the presence of noise, Institute of Radio Engineers 37 (1) (1949).

[27] P. Swain, A. Longtin, Noise in genetic and neural networks, Chaos 16 (2006).

[28] H.C. Tuckwell, Introduction to Theoretical Neurobiology, Cambridge University Press, NY, 1988.

[29] G.E. Uhlenbeck, L.S. Ornstein, On the theory of the Brownian motion, Physical Review 36 (5) (1930).

[30] N.G. van Kampen, Stochastic Processes in Physics and Chemistry, North Holland Eds., 1981.

[31] A. Yakovlev, D. Pivonka, T.H. Meng, A.S.Y. Poon, A mm-sized wirelessly powered and remotely controlled locomotive implantable device, in: Proc. IEEE ISSCC, 2012. February.
[32] A. Yakovlev, S. Kim, A.S.Y. Poon, Implantable biomedical devices: wireless powering and communication, IEEE Communications Magazine 50 (4) (2012).

Laura Galluccio received her Ph.D. in Electrical, Computer and Telecommunications Engineering in March 2005. In 2005 she was a Visiting Scholar at the COMET Group, Columbia University, NY. Since 2002 she has been with the CNIT where she worked as a Research Fellow within the FIRB VICOM and NoE Satnex Projects. She is currently Assistant Professor at University of Catania. Her research interests include ad hoc and sensor networks, protocols and algorithms for wireless networks, network performance analysis and nanonetwork communications.

She serves in the EB of Wiley Wireless Communications and Mobile Computing and Elsevier Ad Hoc Networks Journal and is involved in the TPCs of many top level international conferences. She is also Guest Editor for the Special Issues of IEEE Wireless Communications Magazine on "Wireless communications at the nanoscale" and Elsevier Ad Hoc Network Journal on "Cross-Layer Design in Ad Hoc and Sensor Networks".

Sergio Palazzo was born in Catania, Italy, on December 12, 1954. He received his degree in electrical engineering from the University of Catania in 1977. Until 1981, he was at ITALTEL, Milano, where he was involved in the design of operating systems for electronic exchanges. He then joined CREI, which is the center of the Politecnico di Milano for research on computer networks. Since 1987 he has been at the University of Catania, where is now a Full Professor of Telecommunications Networks. In 1994, he spent the summer at the International Computer Science Institute (ICSI), Berkeley, as a Senior Visitor. He is a recipient of the 2003 Visiting Erskine Fellowship by the University of Canterbury, Christchurch, New Zealand. Since 1992, he has been serving on the Technical Program Committee of INFOCOM, the IEEE Conference on Computer Communications. He has been the General Chair of some ACM conferences, including MobiHoc 2006 and MobiOpp 2010, and currently is a member of the MobiHoc Steering Committee. He has also been the TPC Co-Chair of the IFIP Networking 2011 conference. Moreover, in the recent past, he has been the Program Co-Chair of the 2005 International Tyrrhenian Workshop on Digital Communications, focused on "Distributed Cooperative Laboratories: Networking, Instrumentation, and Measurements", the General Vice Chair of the ACM MobiCom 2001 Conference, and the General Chair of the 2001 International Tyrrhenian Workshop on Digital Communications, focused on "Evolutionary Trends of the Internet". He currently serves the Editorial Board of the journal Ad Hoc Networks. In the recent past, he also was an Editor of IEEE Wireless Communications Magazine (formerly IEEE Personal Communications Magazine), IEEE/ACM Transactions on Networking, IEEE Transactions on Mobile Computing, Computer Networks, and Wireless Communications and Mobile Computing. He was a Guest Editor of Special Issues in the IEEE Journal of Selected Areas in Communications ("Intelligent Techniques in High-Speed Networks"), in the IEEE Personal Communications Magazine ("Adapting to Network and Client Variability in Wireless Networks"), in the Computer Networks journal ("Broadband Satellite Systems: a Networking Perspective"), in the EURASIP Journal on Wireless Communications and Networking ("Ad Hoc Networks: Cross-Layer Issues", and "Opportunistic and Delay Tolerant Networks"). He also was the recipient of the 2002 Best Editor Award for the Computer Networks journal. His current research interests include mobile systems, wireless and satellite IP networks, intelligent techniques in network control, multimedia traffic modeling, and protocols for the next generation of the Internet.

G. Enrico Santagati received his B.S. degree in Telecommunication Engineering and his M.S. degree in Telecommunication Engineering at the University of Catania in 2007 and 2012, respectively. He is currently a Ph.D. student at the University of Buffalo, NY. His research interests include nanomachine communications, ultrasonic communications and green networking.